Contents lists available at SciOpen

Food Science and Human Wellness

journal homepage: https://www.sciopen.com/journal/2097-0765

Elaidic acid-induced intestinal barrier damage led to gut-liver axis derangement and triggered NLRP3 inflammasome in the liver of SD rats

Hui Liu[a,b], Xuenan Li[a], Lu Li[a], Yucai Li[a], Haiyang Yan[a], Yong Pang[a], Wenliang Li[a], Yuan Yuan[a,*]

[a] College of Food Science and Engineering, Jilin University, Changchun 130062, China
[b] School of Public Health, Jining Medical University, Jining 272067, China

ARTICLE INFO

Article history:
Received 21 April 2022
Received in revised form 24 September 2022
Accepted 4 December 2022

Keywords:
Elaidic acid (EA)
Gut microbiota
Intestinal barrier
Gut-liver axis
TLR4-MyD88-NF-κB/MAPK pathways
NLRP3 inflammasome

ABSTRACT

Previous studies have shown that *trans* fatty acids (TFA) are associated with several chronic diseases, the gut microbiota is directly influenced by dietary components and linked to chronic diseases. Our research investigated the effects of elaidic acid (EA), a typical TFA, on the gut microbiota to understand the underlying mechanisms of TFA-related chronic diseases. 16S rDNA gene sequencing on faecal samples from Sprague-Dawley rats were performed to explore the composition change of the gut microbiota by EA gavage for 4 weeks. The results showed that the intake of EA increased the abundance of well-documented harmful bacteria, such as Proteobacteria, *Anaerotruncus*, *Oscillibacter* and Desulfovibrionaceae. Plus, EA induced translocation of lipopolysaccharides (LPS) and the above pathogenic bacteria, disrupted the intestinal barrier, led to gut-liver axis derangement and TLR4 pathway activation in the liver. Overall, EA induced intestinal barrier damage and regulated TLR4-MyD88-NF-κB/MAPK pathways in the liver of SD rats, leading to the activation of NLRP3 inflammasome and inflammatory liver damage.

1. Introduction

Trans fatty acids (TFAs) are unsaturated fatty acids that contain at least one non-conjugated double bond in the trans configuration[1]. Widely used in baked goods, French fries, chocolate, ice cream and other processed foods, industrial TFAs can improve the texture and the flavour, and extend the shelf life[2]. However, TFAs have adverse effects on human health, likely leading to cardiovascular disease, inflammation, neurodegenerative diseases, diabetes and obesity[3-5]. *Trans*-octadecenoic acid isomers account for 80%−90% of the total TFA content, with elaidic acid (EA, $C_{18:1}$ *trans*-9) up to 50% of the total[6-7]. EA can cause elevated total serum cholesterol and low density lipoprotein, which might lead to the development of thrombosis, heart disease and cardiovascular disease[8-9].

TFA intake was reported to increase the abundance of intestinal Proteobacteria compared to saturated fatty acid diets, exacerbating metabolic diseases such as diabetes and fatty liver[10]. TFA intake also increased the abundance of "harmful" bacteria, such as Proteobacteria and Desulfovibrionaceae, whereas it decreased relative abundance of "beneficial" bacteria, such as Bacteroidetes, Lachnospiraceae and Bacteroidales[11]. The liver and the intestine are connected through a bidirectional interconnection of the gut-liver axis[12]. The liver is an endocrine gland that secretes bile acids into the intestine to maintain the stability of the gut microbiota. Excessive bile acid accumulation in the liver and serum can lead to liver damage or even necrosis and thus increase inflammatory damage to the liver[13]. Reduced bile acids in the intestine can lead to intestinal dysbiosis, which impairs intestinal

* Corresponding author at: College of Food Science and Engineering, Jilin University, Changchun 130062, China.
E-mail address: yuan_yuan@jlu.edu.cn (Y. Yuan)
Peer review under responsibility of Tsinghua University Press.

Publishing services by Tsinghua University Press

http://doi.org/10.26599/FSHW.2022.9250107

barrier function, and it has been found that intestinal mucosal barrier dysfunction can lead to translocation of intestinal bacteria, mainly gram-negative bacteria and their product lipopolysaccharides (LPS)[14]. Toll-like receptors (TLR) could explain how the microbiota affects gut motility and the gut-liver axis, as TLR activation mediates intestinal and liver disease in the presence of a compromised intestinal barrier. Endotoxin activates the TLR4/MyD88 pathway by binding to TLR receptors, activating hepatic innate immunity and the expression of various pro-inflammatory cytokines in the liver, leading to chronic liver injury[15-17].

The NLRP3 inflammasome as an intracellular pattern recognition receptor has been shown to be associated with intestinal barrier integrity, microbial composition and liver injury[18-19]. NLRP3 inflammasome are large multiprotein complexes that recognize a variety of microbial, stress and danger-related signals and subsequently trigger the maturation of pro-inflammatory cytokines (IL-1β and IL-18) that promote innate immunity[20]. While IL-18 has been shown to be associated with regulation of the gut microbiota[18]. In summary, NLRP3 inflammasome is associated with the gut-liver axis and modulates liver inflammation by affecting the intestinal mucosal barrier and microbial composition. However, most previous studies have focused on the role of NLRP3 inflammasome in the gut or liver, neglecting its complex role in the intestinal-liver axis.

Gut microbiota plays an important role in the gut-liver axis[21]. Experimental models suggested that intestinal dysbiosis led to intestinal inflammation and mucosal leakage, which caused the translocation of several inflammatory bacterial products[22]. Food compositions have a big impact on the gut microbiota, but the effects of TFAs intake on intestinal microbes are rarely reported. Investigating the effects of EA on the gut-liver axis can help to study the effects of TFAs on the liver and the intestinal innate immune system, and provide insight into the mechanisms of EA-induced inflammatory responses in the body.

2. Materials and methods

2.1 Materials

EA (C18:1T, CAS 112-79-8, purity > 99%) was purchased from ANPEL Laboratory Technologies Co., Ltd. (Shanghai, China). Thirty-six male Specific pathogen-free (SPF) Sprague-Dawley (SD) rats (8 weeks old and weighing 200 g) were purchased from Liaoning Changsheng Biotechnology Co., Ltd. ELISA kits for IL-6, IL-18, IL-1β, tumor necrosis factor-α (TNF-α), and LPS were purchased from USCN KIT Inc. (Wuhan, China). The enzymatic assay kits for lactate dehydrogenase (LDH), alanine aminotransferase (ALT) and aspartate aminotransferase (AST) were purchased from Nanjing Jiancheng Bioengineering Institute (Nanjing, China). IgG secondary antibodies were bought from Bioss Antibodies (Beijing, China). The specific antibodies were displayed in Table 1.

Table 1
Specific antibodies used for Western blotting.

Antibody name	Dilution ratio	Antibody name	Dilution ratio
Claudin-1	1:1 000	JNK	1:1 000
Occludin	1:1 000	p-JNK	1:1 000
ZO-1	1:1 000	p38	1:1 000
MyD88	1:1 000	p-p38	1:1 000
TLR4	1:1 000	ERK	1:1 000
IκBα	1:1 000	p-ERK	1:1 000
p-IκBα	1:1 000	NLRP3	1:1 000
IKK	1:1 000	ASC	1:500
p-IKK	1:1 000	Caspase-1	1:1 000
p65	1:1 000	IL-1β	1:1 000
p-p65	1:1 000	GAPDH	1:10 000

Note: Claudin-1, Occludin, ZO-1, MyD88 and TLR4 were purchased from Affinity Biosciences (OH, USA); p-IκBα, p-IKK and p-p65 were bought from Cell Signaling Technology (Boston, USA); IκBα and p65 were purchased from Proteintech Group (Chicago, USA); IKK, JNK, p-JNK, p38, p-p38, ERK, p-ERK, NLRP3, ASC, caspase-1, IL-1β and GAPDH were bought from Abcam (Cambridgeshire, UK).

2.2 Animals and experimental design

The experiments were implemented in conformity to the Guideline for Animal Experimentation of Jilin University (Changchun, China). The experimental procedures were approved by the Ethical Welfare Committee of Jilin University (No. SY202105011). After adaptive feeding for 1 week, 36 male rats were randomly divided into 4 groups: (i) a negative control group which was given gavage corn oil with 1.0 mL/100 g BW daily, named the CON group. (ii) EA-exposed groups which received gavage EA in corn oil with 50, 100 and 150 mg/kg BW, named the EA 50 group, the EA 100 group and the EA 150 group, respectively. The dosage was determined as previously described and in literature[10,23]. The experiment was conducted within 4 weeks. All rats were housed 3 per cage in constant environmental conditions (12 h light/dark cycle, 20−25 °C, (55 ± 5)% humidity) and had free access to standard feed and drinking water. The body weight was recorded once a week. The SD rats were anesthetized with sodium pentobarbital and blood was taken from the heart. SD rats were quickly dissected and the organs were taken out and frozen at −80 °C.

2.3 Histopathological observation

Liver and colon tissue were immediately placed in 10% formalin solution for 24 h. Dehydration operations were then carried out with gradient ethanol, clear treatment with xylene, wax immersion in wax cylinders at 63 °C, dewaxing and hydration after embedding the sections (3 μm), which were subsequently stained with hematoxylin and eosin (H&E). The sections were placed under a light microscope (CX22, Olympus, Japan) to monitor the changes in histomorphological structure.

2.4 Transmission electron microscopic observation

Colon tissue was immediately fixed in 2.5% glutaraldehyde overnight at 4 °C and then infiltrated with PBS solution overnight. The sections were fixed in 1% osmium solution for 2 h at 4 °C, dehydrated with graded ethanol and acetone and then embedded in a medium consisting of embedding agent and acetone. Staining of ultrathin sections was done with dioxygen acetate and lead citrate, and

finally the ultrastructure of tissue was observed under a JEM 1400 (JEOL Ltd., Japan) transmission electron microscope at 80 kV.

2.5 Measurements of biochemical parameters

The release of IL-1β, IL-18, IL-6, TNF-α and LPS in liver or colon of SD rats were detected using rat ELISA kits according to the protocol. Liver or colon of SD rats was ground and centrifuged to collect the supernatant (4 °C, 10 000 × *g* for 5 min). The activity of LDH, ALT and AST were assayed using commercial kits according to the manufacturer's instructions. Rat blood was allowed to stand for 4 h at room temperature and then centrifuged to collect the supernatant (4 °C, 630 × *g* for 10 min). Liver or colon was homogenized with saline buffer at a ratio of 1:9, and then centrifuged to obtain tissue homogenate (4 °C, 630 × *g* for 10 min).

2.6 Real-time quantitative PCR (RT-qPCR)

Total RNA was extracted from liver tissue homogenate using Simply P Total RNA Extraction kit (BioFlux, Beijing, China). The concentrations of RNA were determined by UV spectrophotometer. RNA (1 μg) was reverse-transcribed to complementary DNA (cDNA) via PrimeScript RT reagent kit (Monad Biotechnology Co., Ltd., Suzhou, China). The sequences of specific primers employed and the subsequent steps were based on our previous experiments[24].

2.7 Western blotting analysis

Rat tissue was mixed with RIPA lysis buffer (containing 1% protease and 1% phosphatase inhibitor) at a ratio of 1:10 and homogenised thoroughly, then centrifuged at 10 010 × *g* for 10 min at 4 °C. The supernatant was taken as protein preparation solution. Protein content determination and Western blotting were conducted as mentioned in our previous study[24].

2.8 Gut microbiota analysis

Five samples of each group were randomly selected and thawed. DNA was extracted from the samples using the E.Z.N.A.® Stool DNA Kit (D4015, Omega, Inc., USA) following the manufacturer's instructions. The resulting PCR products were purified by AMPure XT beads (Beckman Coulter Genomics, Danvers, MA, USA) and Qubit (Invitrogen, USA) was used for quantification, and the document was obtained after evaluating on 2100 Bioanalyzer (Agilent, USA) and Illumina (Kapa Biosciences, Woburn, MA, USA) library quantification kits. The gut microbiota profile was determined using a MiSeq high-throughput sequencing platform (NovaSeqPE250) according to the manufacturer's recommendations, provided by LC-Bio Technology Co., Ltd. (Hangzhou, Zhejiang Province, China). Quality filtering of raw reads under specific filtering conditions to obtain high quality CLEAN tags according to fqtrim (v0.94). Filtering of the chimeric sequences was performed using Vsearch software (v2.3.4). Demodulation was performed using DADA2 to obtain feature tables and feature sequences. Diversity was calculated by normalizing to the same random sequence. Feature abundance was then normalized using the relative abundance of each sample according to the SILVA (release 132) classifier. Alpha and Beta diversity were calculated by QIIME2 and plotted by the R package. Sequence comparison was performed using Blast, and each representative sequence was annotated with the SILVA database for the feature sequences. Other plots were implemented using the R package (v3.5.2).

2.9 Statistical analysis

Experimental data were expressed as the mean ± SD of three independent replicate experiments, and analyzed by ANOVA and Newman-Keuls multiple comparison tests. GraphPad Prism 7 (GraphPad Software, Inc., La Jolla, USA) was used for statistical analysis and plotting. Difference between the mean values was considered significant at $P < 0.05$. Quantitative analysis of the Western blot bands was performed using Image J software.

3. Results

3.1 EA induced intestinal damage in SD rats colon

The results of H&E staining in the colon of SD rats were shown in Fig. 1A. The CON group featured neatly arranged intestinal epithelial cells, normal crypt structure, and clear intermediate glands,

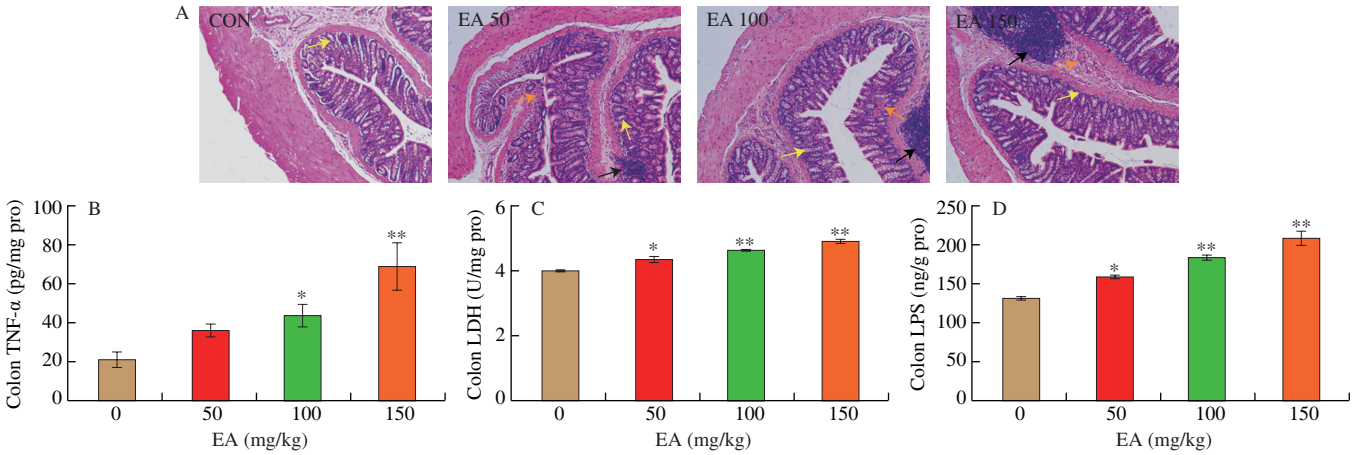

Fig. 1 EA induced intestinal damage in SD rats colon. (A) The histopathological changes of colon (100×). Yellow arrow shows abnormal crypt structure, red arrow represents red blood cells, black arrow represents inflammatory cells. (B) EA induced the release of TNF-α in colon. (C) EA induced the increase of LDH level in colon. (D) EA induced the increase of LPS level in colon. Significant differences with the CON group were designated as $*P < 0.05$ or $**P < 0.01$. The same below.

without inflammatory cell infiltration, congestion or edema observed, and the muscle layer and mucosal structure were intact. In contrast, the EA 50 group showed histological disorganization with localized inflammatory cells. Irregularity of the crypt surface, deformation of the intestinal villi and inflammatory cell infiltration were observed in the EA 100 group, while the EA 150 group featured atrophy of the crypt structure, increased inflammatory cells and destruction of the muscular layer with epithelial cell loss.

As the histopathological findings showed significant lesions in the intestinal tissues, the release level of TNF-α was measured in the colon. The result suggested that EA significantly up-regulated the level of TNF-α release in the rat colon compared to the CON group (Fig. 1B, $P < 0.01$). LDH was present in all cells or tissues of the body and its level can reflect the metabolic status of the body. Compared with the CON group, LDH levels in colon of rats showed significant increase in the EA groups (Fig. 1C, $P < 0.01$), demonstrating that EA induced significant lesions in the gut. The result further indicated that EA induced inflammatory damage in rat intestine. Meanwhile, LPS levels in colon of the EA groups were significantly higher compared to the CON group (Fig. 1D, $P < 0.01$), indicating that EA induced a large amount of endotoxin production in rat intestine.

3.2 EA induced intestinal barrier damage in SD rats

Transmission electron microscope (Fig. 2A) showed that the intestinal villi in the CON group were relatively dense and well arranged, with tight junctions intact, dense and continuous, and a high density of bridging grains. In contrast, the EA 50 group had loose tight junctions, significantly widened gaps, decreased density of bridging grains, reduced number of microvilli and more disorganized arrangement. In the EA 100 group, the intestinal villi were disorganized and sparse, with unclear intercellular connections, vacuole formation, partial breakage of tight junctions, open and loose connections. The intestinal villi in the EA 150 group were detached and sparse, with vacuole formation, incomplete tight junctions, decreased density of bridging grains and widened cell gaps. This

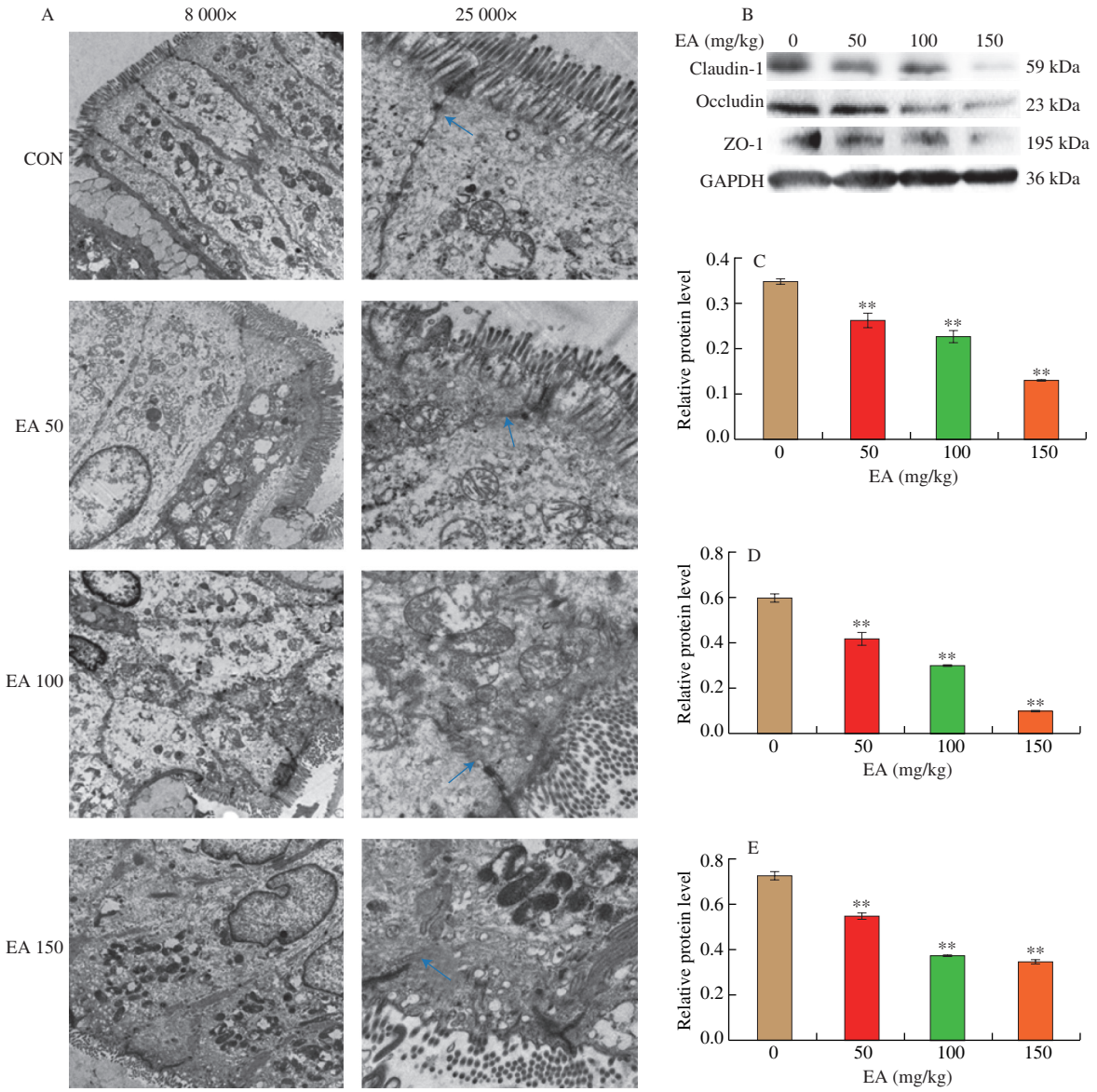

Fig. 2 EA induced intestinal barrier damage in SD rats. (A) Effect of EA on ultrastructure in colon, blue arrow represents tight junction. (B) Western blot image; Gray analysis of (C) ZO-1; (D) Claudin-1; (E) Occludin.

indicated that the intestinal junctions in the rats were disrupted and the intestinal mucosal barrier was damaged by EA.

EA induced a significant increase in the levels of intestinal LPS and the inflammatory factor TNF-α, which would damage the intestinal epithelial barrier and alter the integrity of the intestinal barrier. Pathological histology of the colon also showed disruption of the tight junctions of the intestine. Therefore, the effect of EA on the integrity of the intestinal barrier in rats was investigated by measuring the expression of intestinal tight junction proteins. The results showed that the expressions of ZO-1, Occludin and Claudin-1 were all significantly down-regulated in rat colon compared to the CON group (Figs. 2B-E, $P < 0.01$), indicating that EA induced the increase in intestinal epithelial barrier permeability, with bacteria and their endotoxins entering the circulation, further exacerbating the inflammatory response.

3.3 *EA induced liver injury in SD rats*

H&E staining results (Fig. 3A) showed that in the CON group, the liver tissue cells were tightly arranged, with good lobular structure and without obvious abnormalities. The nucleus was located in the middle of the cells; the hepatic cords were roughly arranged in a radial pattern; the morphology of hepatocytes did not change; there was no vacuolation or inflammatory changes observed. In the EA 50 group, the structure of the liver cords was slightly disordered, there were local inflammatory cell infiltration and a small amount of fat vesicles. In the EA 100 group, disorganized cord structure, vacuole-like changes, abnormal aggregation of red blood cells in the hepatic sinusoids, inflammatory cell infiltration, as well as swollen and deeply stained nuclei were observed in the hepatocytes. In the EA 150 group, the cells had poorly defined hepatic lobules, obstructed red blood cell sludge, massive inflammatory cell infiltration and vacuole-like degeneration, deviated nuclei position, blurred cell boundaries, and obvious inflammatory damage. Overall, histological examination revealed significant pathological damage to the liver.

Compared with the CON group, LDH levels of serum and liver increased significantly in EA groups (Figs. 3B-C, $P < 0.05$, $P < 0.01$), demonstrating that EA induced significant lesions in the rat organism. In addition, LPS levels were significantly higher than that in the CON group (Figs. 3D-E, $P < 0.05$, $P < 0.01$), indicating EA induced translocation of endotoxin produced in the rat intestine to the liver and circulatory system. ALT and AST tests are normally used to assess liver function or the extent of liver injury, and patients with chronic hepatitis exhibit elevated serum transaminases. The results

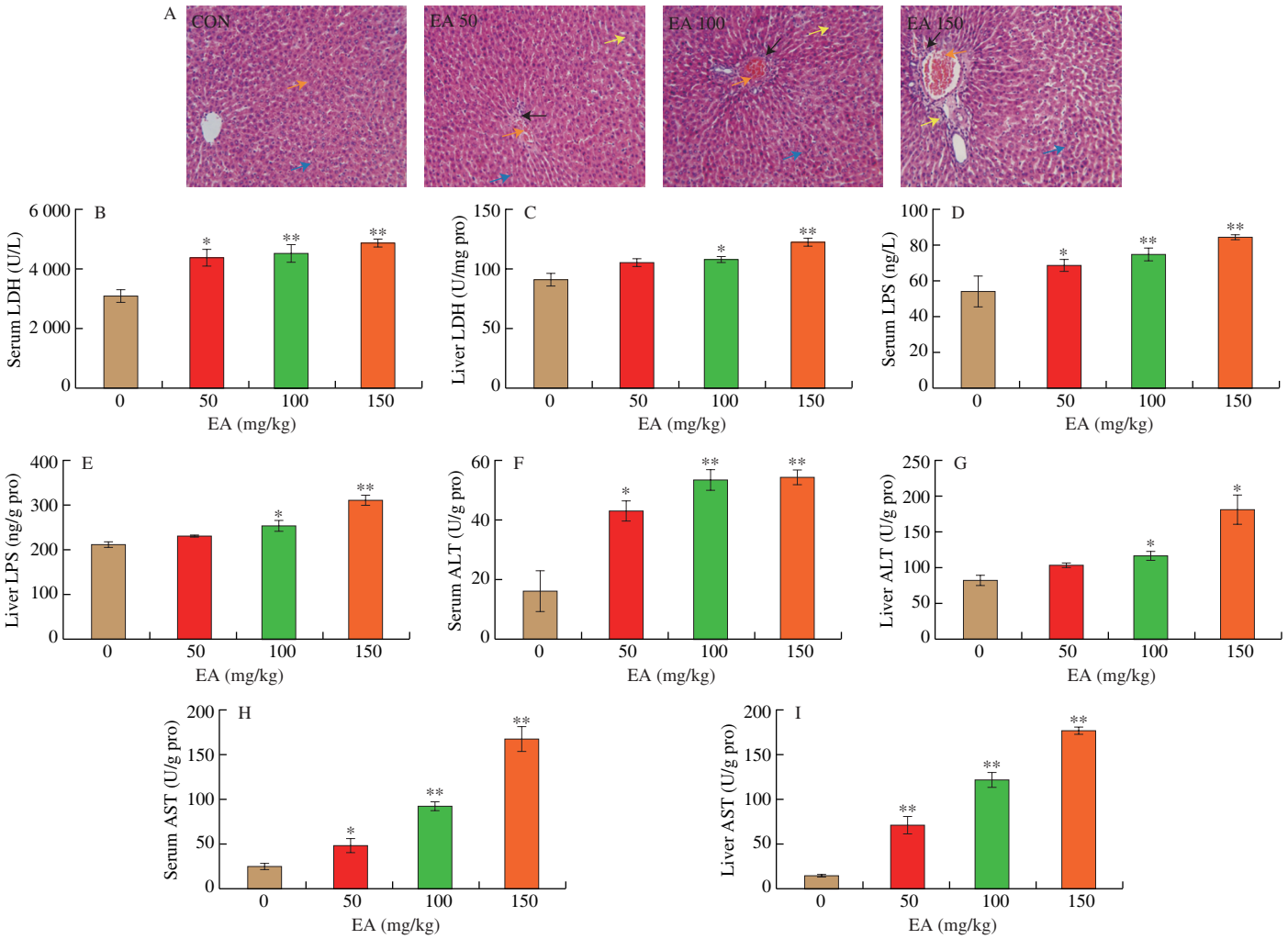

Fig. 3 EA induced liver injury in SD rats. (A) The histopathological changes of liver (100×). Yellow arrow shows cavitation, red arrow represents red blood cells, black arrow represents inflammatory cells, blue arrow represents the nucleus. (B, C) EA induced the increase of LDH level in serum and liver. (D, E) EA induced the increase of LPS level in serum and liver. (F, G) EA induced the increase of ALT level in serum and liver. (H, I) EA induced the increase of AST level in serum and liver.

showed that EA induced a dose-dependent increase in ALT and AST levels in both liver and serum compared to the CON group (Figs. 3F-I, $P < 0.05$, $P < 0.01$), thus indicating that EA induced liver injury and inflammatory response in SD rats.

3.4 Effect of EA on gut microbiota of SD rats

3.4.1 Alpha and beta diversity analysis

Chao1 and Observed_otus index mainly reflect species richness information of samples. Chao1 (Fig. 4A) and Observed_otus index (Fig. 4B) indicated that there was a significant difference in species richness between EA 50 and EA 150 groups, EA 100 and EA 150 groups. The Simpson and Shannon indices were used to represent species richness and evenness. The Shannon index (Fig. 4C) showed significant differences between the EA 150 group and the other three groups, while the Simpson index (Fig. 4D) showed significant differences between CON and EA 100 groups, CON and EA 150 groups, EA 50 and EA 150 groups.

Beta diversity refers to the variability of species between different environmental communities. In this study, principal coordinate analysis (PCoA) was used to compare differences in microbial composition between samples (Fig. 4E). Significant differences were found between the EA 150 group and the other three groups in terms of gut microbiota. As shown from the diversity results, the species composition of these 4 groups varied considerably.

3.4.2 Microbial community structures at the phylum and genus levels

Superimposed histograms demonstrating the structure of the gut microbiota illustrated the distribution and relative abundance of microbial species at each level. At the phylum level (Fig. 5A), Firmicutes, Bacteroidetes, Proteobacteria, and Actinobacteria were dominant in each group. Different doses of EA had different effects on the gut microbiota of rats. Compared to the CON group, a decrease in Patescibacteria was observed in the EA 50 group while a decrease in Epsilonbacteraeota and Proteobacteria was seen in the EA 100 group. The abundance of Patescibacteria, Epsilonbacteraeota and Firmicutes decreased significantly in the EA 150 group, while the abundance of Verrucomicrobia, Proteobacteria and Actinobacteria were higher than that in the CON group. The abundance of Proteobacteria and Actinobacteria were significantly higher in the EA 150 group compared to the EA 50 and EA 100 groups.

At the genus level (Fig. 5B), the distribution of the gut microbiota was significantly altered among the 4 groups. The EA 50 group

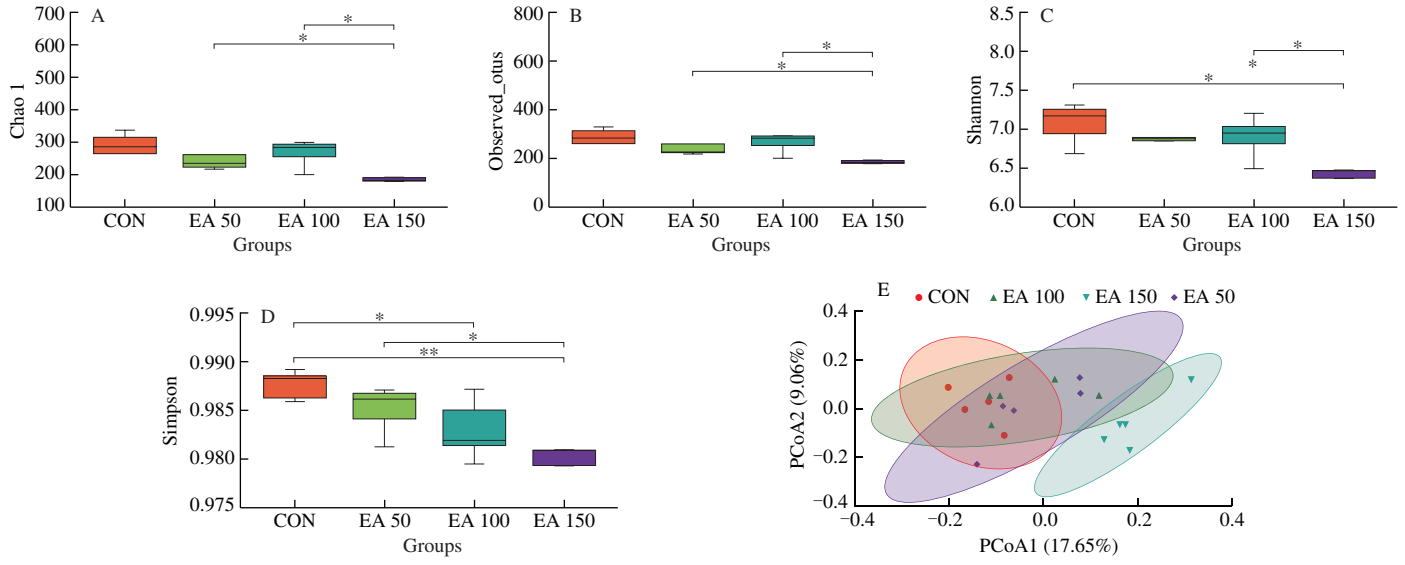

Fig. 4 Alpha and beta diversity analysis. Alpha diversity analysis of species distribution including the (A) Chao1, (B) Observed_otus, (C)Shannon and (D) Simpson. (E) PCoA analysis among all the groups ($P = 0.001$). *$P < 0.05$, **$P < 0.01$.

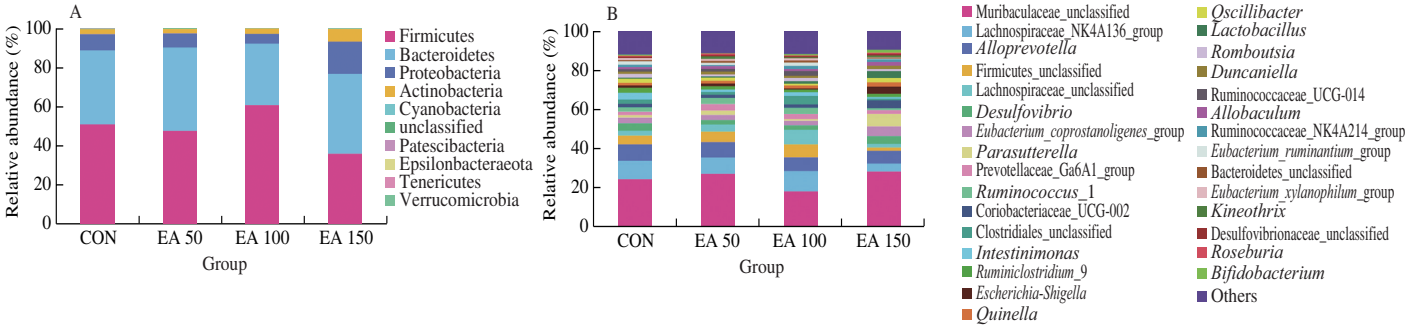

Fig. 5 Differences of microbial community structures at the phylum and genus levels. (A) Column of microbial at phylum level in each group; (B) Column of microbial at genus level in each group.

showed a significant decrease in the abundance of *Candidatus_Saccharimonas*, *Pygmaiobacter*, *Intestinimonas*, *Ruminiclostridium_9* and *Peptococcus*, and the abundance of *Anaerotruncus* was higher than that in CON. *Helicobacter*, *Ruminiclostridium_9*, *Oscillibacter*, *Intestinimonas* and *Peptococcus* were significantly down-regulated in the EA 100 group administration, and the relative abundance of Erysipelotrichaceae_unclassified increased significantly compared to the CON group. At the same time, the abundance of *Helicobacter*, *Acetatifactor*, *Candidatus_Saccharimonas*, *Ruminiclostridium*, Ruminococcaceae_UCG-014, *Intestinimonas*, and *Peptococcus* in EA 150 were lower than that in CON, while *Dubosiella*, *Parabacteroides*, *Parasutterella*, *Lactobacillus*, *Anaerotruncus*, *Olsenella*, *Peptococcus*, *Burkholderia-Caballeronia-Paraburkholderia* increased significantly in abundance.

3.4.3 LEfSe analysis

In the LEfSe analysis (Fig. 6), the effects of biomarkers in different species were evaluated by linear discriminant analysis (LDA). The dominant bacteria in the control group were *Helicobacter* of Epsilonbacteraeota, *Intestinimonas*, *Ruminiclostridium_9*, *Candidatus_Saccharimonas* of Patescibacteria. Prevotellaceae_UCG_001, *Ruminococcus* were identified as the major flora in the EA 50 group. Christensenellaceae, Ruminococcaceae, *Clostridia* and Firmicutes were found to be the dominant bacteria in the EA 100 group. While in the EA 150 group, Actinobacteria, Proteobacteria, *Olsenella*, *Lactobacillus*, *Anaerotruncus*, *Oscillibacter*, *Dubosiella*, *Desulfovibrio* and Burkholderiaceae were dominant microbiota.

3.5 Effects of EA on TLR4/MyD88 signalling pathway in the liver of SD rats

The above results suggested that EA-induced endotoxin translocation in rats triggered disruption of gut microbiota and damage to the intestinal epithelial barrier, which could lead to translocation of LPS into the hepatic circulation and further exacerbate the liver inflammatory response. TLR4 is an important ligand for LPS that could specifically recognize endotoxins. Therefore, to explore whether EA-induced liver inflammation in relation to the TLR4 pathway, the expression levels of TLR4/MyD88 signalling pathways-related proteins in liver were further examined. As shown in Fig. 7, the expression levels of TLR4 and MyD88 were significantly increased ($P < 0.05$, $P < 0.01$). The phosphorylation levels of the NF-κB signalling pathway-related proteins IκB, IKK and p65 were all increased with statistical differences ($P < 0.05$, $P < 0.01$). Meanwhile, the expression levels of the MAPK signalling pathway-related proteins p-JNK, p-ERK and p-p38 were significantly up-regulated ($P < 0.05$, $P < 0.01$) in a dose-dependent manner in EA groups compared with CON. The above results demonstrated that EA induced the activation of TLR4-MyD88-NF-κB/MAPK signaling pathways in rat liver via LPS and pathogenic bacteria, thereby triggering the liver inflammatory response.

3.6 Effect of EA on NLRP3 inflammasome activation in the liver of SD rats

NLRP3 inflammasome activation is closely associated with the inflammatory response. To investigate the effect of EA on the activation of NLRP3 inflammasome in the liver of SD rats, mRNA expression levels of *NLRP3*, *caspase-1*, *ASC* and *IL-1β* in the rats liver were firstly examined using RT-qPCR. The results in Fig. 8 showed that mRNA expression levels of *NLRP3*, *caspase-1*, *ASC* and *IL-1β* in liver of EA groups were significantly increased compared to the CON group ($P < 0.05$, $P < 0.01$), indicating that EA intervention likely induced NLRP3 inflammasome activation in rat liver. The speculation was confirmed at the protein level, where the protein expression levels of NLRP3, ASC, IL-1β and Cleaved Caspase-1 were significantly increased in a dose-dependent manner in EA groups compared to CON group (Fig. 9, $P < 0.05$, $P < 0.01$). The results indicated that EA induced NLRP3 inflammasome activation in the liver of SD rats.

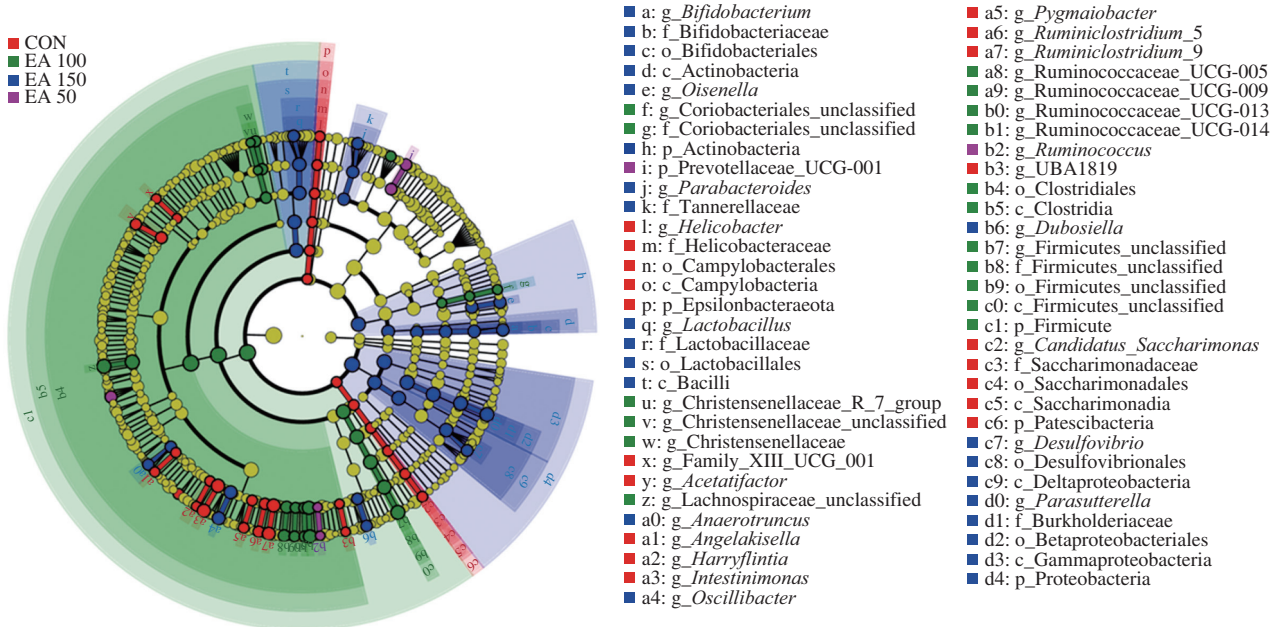

Fig. 6 Evolutionary branch maps of LEfSe analysis.

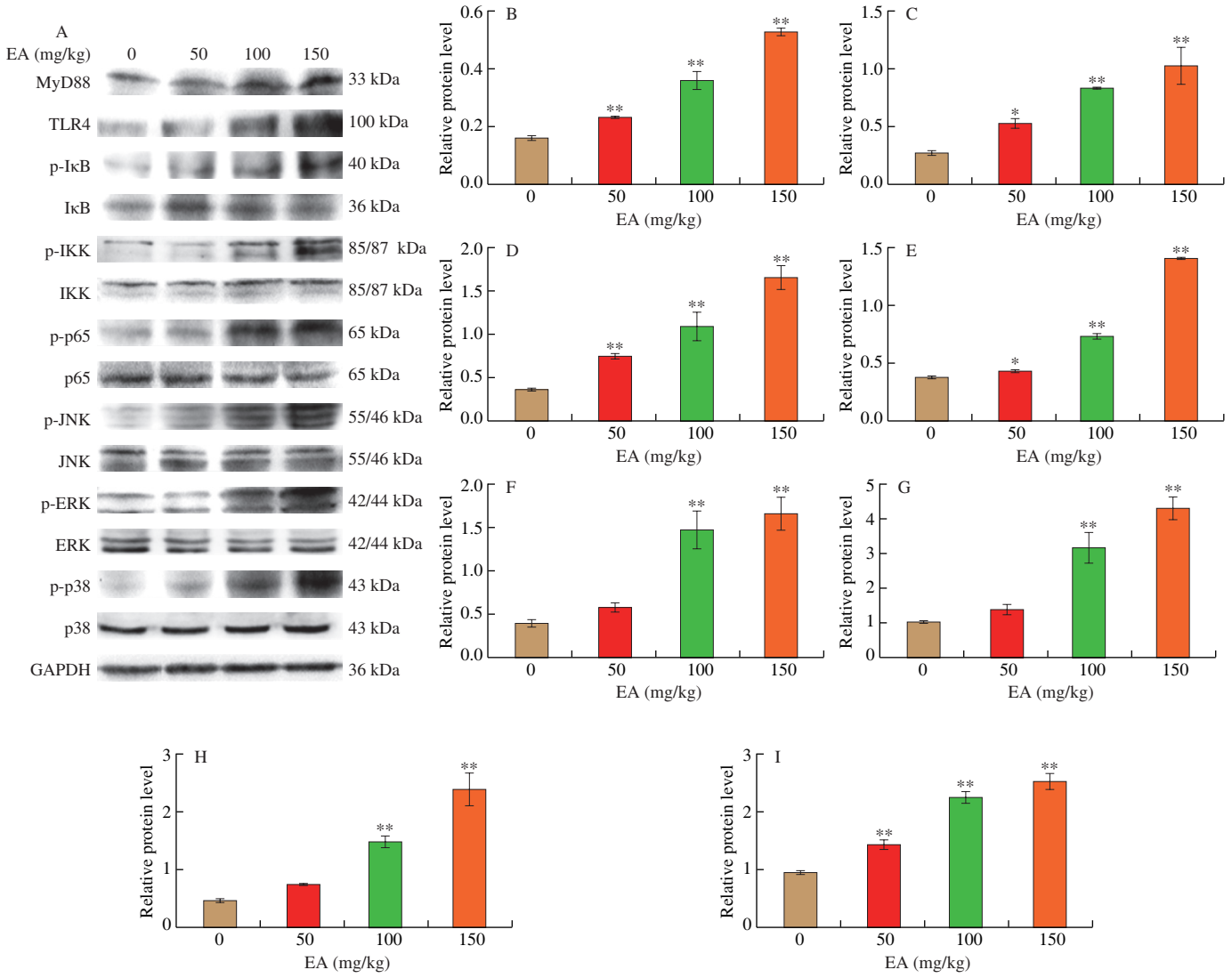

Fig. 7 Effects of EA on expression levels of TLR4 /MyD88 pathway in SD rats liver. (A) Western blot image; Gray analysis of (B) TLR4, (C) MyD88, (D) p-IκB/IκB, (E) p-IKK/IKK, (F) p-p65/p65, (G) p-ERK/ERK, (H) p-JNK/JNK, (I) p-p38/p38.

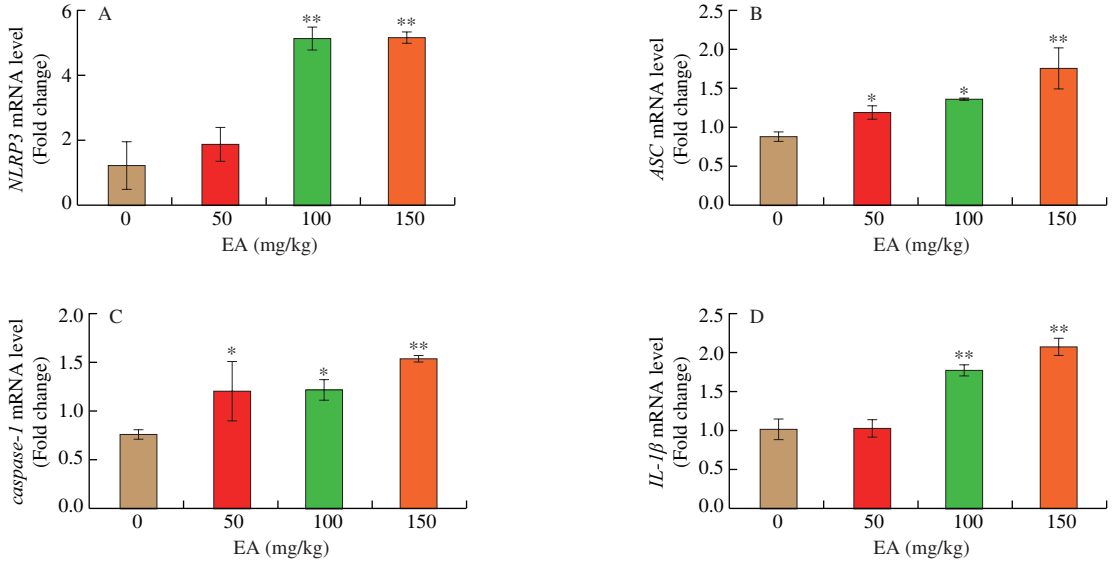

Fig. 8 Effects of EA on mRNA expression levels of the NLRP3 inflammasome-related proteins in SD rat livers. (A) *NLRP3*; (B) *ASC*; (C) *caspase-1*; (D) *IL-1β*.

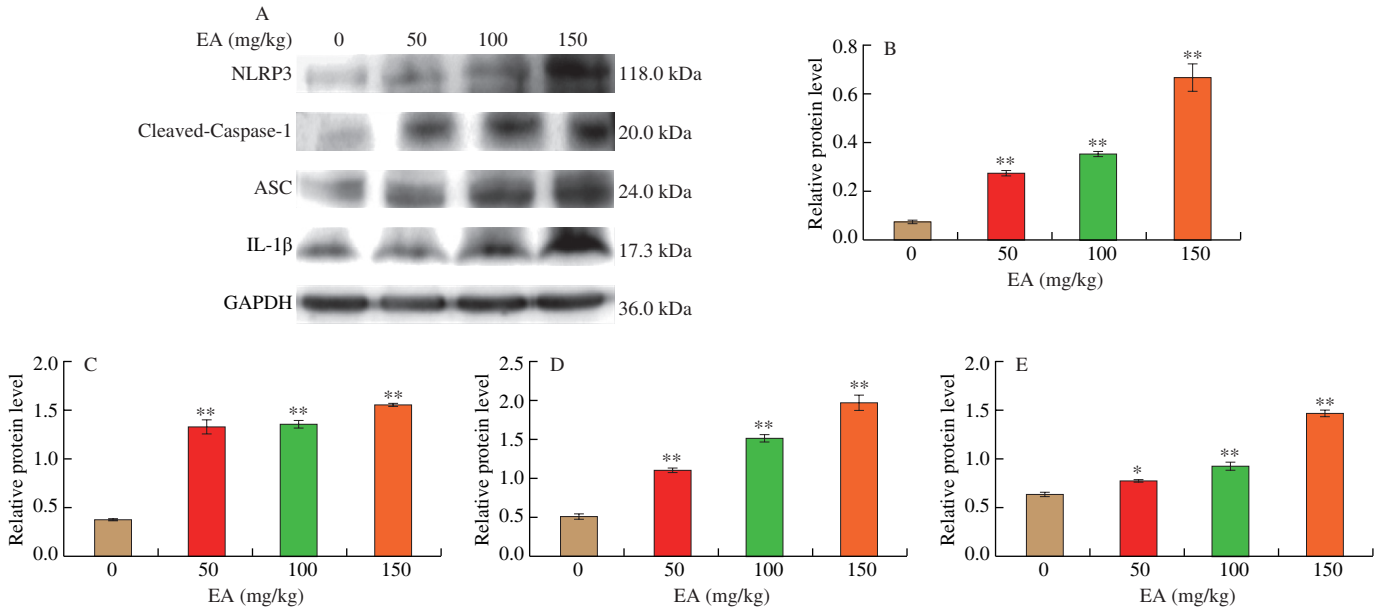

Fig. 9 Effects of EA on expression levels of NLRP3 inflammasome-related proteins in SD rats liver. (A) Western blot image; Gray analysis of (B) NLRP3, (C) Caspase-1, (D) ASC, (E) IL-1β.

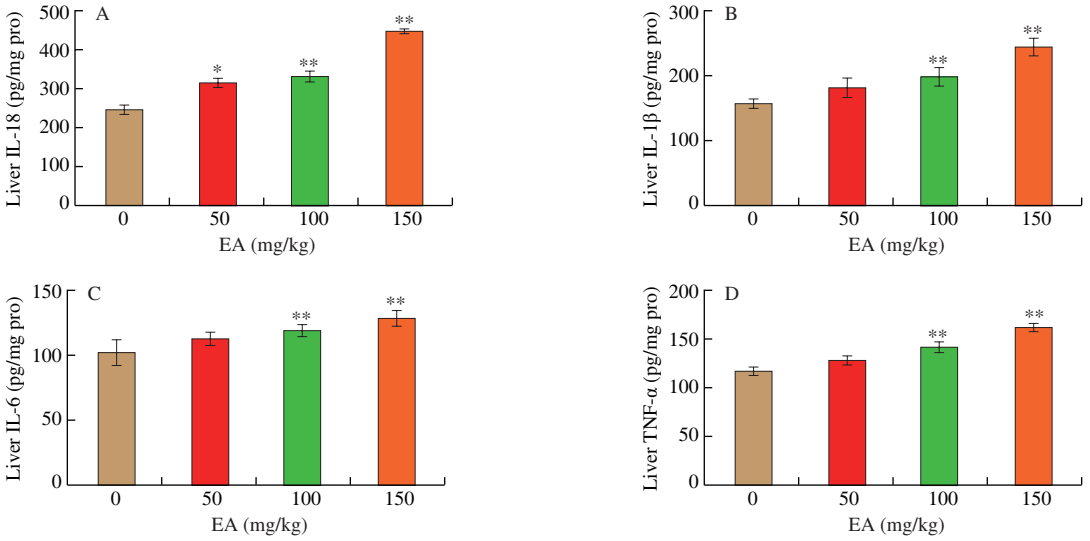

Fig. 10 Effects of EA on the release of inflammatory factors from SD rats liver. (A) Liver IL-18; (B) Liver IL-1β; (C) Liver IL-6; (D) Liver TNF-α.

Levels of inflammatory cytokines in liver respond to the level of systemic inflammation and the state of immune activation in rats. When the NLRP3 inflammasome was activated in rat liver, the organism underwent the inflammatory response and induced the release of inflammatory factors. The expressions of inflammatory factors in rat liver were shown in Fig. 10, compared with the CON group, the expression levels of IL-18, IL-1β, IL-6 and TNF-α were significantly increased in a dose-dependent manner in EA-induced group ($P < 0.05$, $P < 0.01$). To sum up, EA induced NLRP3 inflammasome activation in the liver of SD rats and released large amounts of inflammatory factors.

4. Discussion

To varying degrees, dietary lipids and fatty acids affect intestinal microbiota. However, little is known about the effects of TFAs on the intestinal tract. As EA is the main isomer of TFAs, the aim of this study was to investigate the effect of EA on the intestine of SD rats. The largest EA dose (150 mg/kg) used in rats was converted to a human equivalent dose of 24.32 mg/kg, which is comparable to 1 824 mg EA in a 75 kg human. This concentration may be provided through a daily diet supplement. The World Health Organization (WHO) recommends that TFAs intake be limited to less than 1% of total energy intake (approximately 2 200 mg of TFAs). At the same time, we also analyzed and discussed other related studies. In the studies of de Brito Medeiros et al.[23] and Okamura et al.[10], the intake of EA was above the restricted consumption level. We hypothesize that the use of higher experimental doses may be an attempt to more accurately determine the mechanism and extent of damage caused by TFAs to the organism. We would like to emphasize that an appropriately calculated dose based on research in rat is achievable in humans. However, we advocate that TFAs should be avoided in the diet as much as possible.

The results of H&E staining and transmission electron microscopy showed that EA caused significant pathological damage to the rat colon compared with CON group, and the most severe damage was caused by high dose of EA. LDH levels, an important marker for disease assessment, are significantly increased in diseases such as pneumonia and tumours[25]. When tissues and organs are damaged, LDH levels in serum and related tissues increased significantly. The results demonstrated that EA induced a significant increase in LDH levels in liver, colon and serum, indicating damage occurred to both liver and intestine. At the same time the ELISA results indicated that EA induced a significant release of TNF-α in the rat colon. TNF-α is an inflammatory mediator essential to the process of systemic inflammatory response, which can modulate the immune system, as well as the synthesis and release of other cytokines. The above results demonstrated that EA induced inflammatory damage in the intestine. Okamura et al.[10] found significant inflammatory damages in the pathological tissue of the small intestine in mice fed TFAs, with significantly increased expression levels of inflammatory factors such as TNF-α, IL-6 and IL-1β in the liver and small intestinal mucosa, promoting the accumulation of liver fat and development liver fibrosis.

The liver and the intestine are connected through a bidirectional interconnection of the gut-liver axis[12]. Dysregulation of intestinal microecology, which impairs intestinal barrier function, induces massive translocation of enteric pathogens and endotoxins into the portal system, creating an extremely complex response that exacerbates intestinal damage and further causes inflammatory damage to other organs such as the liver[15-16]. 16S rDNA analysis showed a significant decrease in the EA-induced group compare to CON group in the abundance of *Intestinimonas*, which was important butyrate producers in the human microbiota[26]. An increased abundance of Prevotellaceae_UCG_001 was found in the EA 50 group, and the abundance of this genus may lead to depression[27].

The intestinal microorganisms that were significantly different from the other groups in the EA150 group were Actinobacteria, Proteobacteria, *Bifidobacterium*, *Olsenella*, *Lactobacillus*, *Anaerotruncus*, *Oscillibacter*, *Dubosiella*, *Desulfovibrio* and Burkholderiaceae. This suggested that EA intake notably increased the amount of harmful bacteria groups. The abundance of Actinobacteria was significantly increased in patients with nonalcoholic fatty liver disease (NAFLD), and the degree of fatty liver and abnormal liver function were positively correlated with the abundance of the Actinobacteria and the Proteobacteria[28-29]. Proteobacteria are a major source of the intestinal translocation antigen LPS[30-31], and pro-inflammatory bacteria, considered to be a microbial signature of dysbiosis in the gut flora[32]. Gao et al.[33] found that *Anaeroruncus* was associated with intestinal permeability index, LPS and tight junction protein in high-fat diet-fed rats, suggesting its involvement in the loss of barrier function and LPS production. In addition, *Oscillibacter* was enriched in mice with colorectal cancer[34]. *Oscillibacter* was also increased in mice fed a high saturated fat diet, contributing to increased intestinal permeability and negatively correlating with *trans*-epithelial resistance in the proximal colon[35]. Curiously, *Oscillibacter* was the dominant microbiota in the EA 150 group but not in the EA 100 group. This somehow confirmed that the effect of different concentrations of EA on intestinal flora varies greatly, the same conclusion has been obtained in other studies. Ge et al.[11] suggested that there were differences in cecal microbiota composition among the mouse with low partially hydrogenated oil (LH) and high partially hydrogenated oil (HH) diet. According to relative abundance at the family level, Lachnospiraceae from the was the most abundant family in the cecum bacterial communities of LH mice, and the second-most abundant family was Desulfovibrionaceae, which was the same in the control group. However, in HH mice, the ratio of Desulfovibrionaceae was markedly increased and was dominant in cecum bacterial communities. Even more impressively, compared with the control group, higher levels of Lactobacillaceae were found in the LH group than in the HH group. Hua et al.[36] observed no significant differences in the relative abundance of rat gut microbiota at the phylum level, but at the genus level, *Bacteroides* and Muribaculaceae showed different abundances among the TFAs diet groups (1% TFA and 8% TFA). The proportion of genus *Bacteroides* was increased in the 1% TFA groups compared with the CON group, however, the abundance of *Bacteroides* in 8% TFA groups was significantly lower than that in 1% TFA groups. In addition, the proportions of Muribaculaceae in the 1% TFA and 8% TFA groups were lower than that in the CON group, but the abundance of Muribaculaceae in 8% TFA groups was significantly higher than that in 1% TFA groups.

Diets of EA resulted in increased abundance of the Desulfovibrionaceae and *Desulfovibrio*. As gram-negative bacteria, most members of the *Desulfovibrio* are LPS producers that disrupt the intestinal barrier[37]. The increased relative abundance of Desulfovibrionaceae and the resulting excess hydrogen sulphide production may contribute to the development of inflammatory bowel disease (IBD) and inflammation-related intestinal diseases, such as colorectal cancer[38]. Studies have also been reported that increased abundance of Desulfovibrionaceae was associated with obesity[39]. Increase in the abundance of Proteobacteria and Desulfovibrionaceae was also found in TFAs diets[11,40], and these gram-negative bacteria were found to be abundant in obese and metabolically impaired mice[41]. Furthermore, intake of industrial TFAs resulted in increased release of inflammatory factors and decreased production of butyric and valeric acids. Li et al.[42] found that intake of TFAs altered the fatty acid profile of the small intestinal mucosa, in particular inducing excessive accumulation of EA. The relative abundance of Proteobacteria, *Lactobacillus*, *Desulfovibrio*, *Peptostreptococcus* and *Turicibacter* was significantly different in the TFAs diet group compared to the control group.

Surprisingly, EA 150 stimulated the increase in two recognized probiotics, *Lactobacillus* and *Bifidobacterium*. Ge's[11] study echoed our findings and explained the occurrence of this phenomenon, as EA stimulated the growth and multiplication of *Lactobacillus* in the *in vitro* fermentation experiments, while *in vivo* analysis experiments in mice confirmed that EA induced an increase in intestinal *Lactobacillus*. Although *Lactobacillus* has traditionally been considered to be beneficial to health, recent evidence suggested that increased abundance of *Lactobacillus* might be associated with obesity and inflammatory conditions[43]. The count of intestinal *Bifidobacterium* was also found to increase significantly in response to TNF-α stimulation[44]. This may explain the increase in beneficial bacteria *Lactobacillus* and *Bifidobacterium* in the EA group. Hua et al.[36] found that low and high doses of TFAs did not have the same effect on the gut microbiota of rats induced by a high-fat diet. Similar to the findings of the above research, different doses of EA had different effects on the gut microbiota of rats, but the significantly different

abundance of bacteria in each group was all strongly associated with the development of an inflammatory response and disruption of the intestinal barrier.

The close link between the gut and the liver determines the critical regulation of liver health by the intestinal microbiota. The regulatory mechanisms of the gut-liver axis are controlled by the intestinal barrier, the composition of the gut microbiota and normal liver function. When the intestinal mucosal barrier is disrupted by external stimuli, intestinal bacteria and their products migrate through the damaged intestinal barrier to the liver, causing a series of inflammatory responses. The EA-induced harmful bacteria were involved in the loss of barrier function and the production of LPS. LPS is one of the intestinal metabolites and an endotoxin-specific antigen. TLR4 recognizes LPS to induce the release of a variety of inflammatory cytokines, which leads to the inflammatory response. ELISA results showed significant increase in serum, liver and intestinal LPS levels, together with the colonic ultrastructural results, demonstrating that EA induced damage to the intestinal mucosal barrier in rats. In general, liver inflammation is the pathophysiological basis for gut microbiota-associated liver injury[45]. Increased intestinal LPS triggers endotoxaemia, which can lead to increased intestinal permeability and consequently liver inflammation[46]. The gut microbiota can cause liver injury by increasing LPS, which induces liver inflammation and lipid accumulation by activating the NF-κB signalling pathway through TLR4 receptor recruitment of MyD88. TLR4 is a major component of the LPS recognition receptor complex and activation of the TLR4/MyD88 pathway induces the production of pro-inflammatory cytokines such as TNF-α, IL-6 and IL-1β, which play a major role in the inflammatory response to adrenoleukodystrophy (ALD)[47]. Gram-negative bacteria, such as *Prevotella* and *Veillonella*, are significantly increased in the gut in patients with cirrhosis and may be associated with activation of the LPS-TLR4 axis[48]. The above studies suggested that Proteobacteria, *Anaerotruncus*, *Oscillibacter* and *Desulfovibrio* may be responsible for the destruction of intestinal barrier. In addition, increased intestinal permeability and intestinal barrier dysfunction may also play a key role in the development and progression of liver disease[49]. Epithelial cells maintain the stability of the intestinal barrier through tight junction structures, and the expression of tight junction proteins is a major marker of epithelial cell structure and function[50]. The results of this study showed that the expression levels of ZO-1, Occludin and Claudin-1 were significantly down-regulated in the colon in EA-induced groups, indicating that EA induced an increase in intestinal epithelial barrier permeability in rats, resulting in LPS entering the circulation via the broken intestinal lumen and inducing liver inflammation.

Clearly, the expression levels of TLR4 and MyD88 in the liver were significantly increased with EA treatment, demonstrating that EA-induced leakage of intestinal LPS and harmful intestinal bacteria could activate the liver TLR4-MyD88 pathway. NF-κB is a key nuclear transcription factor that regulates innate and adaptive immunity by promoting the expression of pro-inflammatory cytokines, chemokines, enzymes and adhesion molecules[51]. In a model of LPS-induced liver injury, activation of the NF-κB signalling pathway induced NLRP3 inflammasome activation and production of IL-1β, IL-18 and TNF-α[52]. MAPK is closely associated with inflammation and tumourigenesis. Multiple stimuli, including LPS, activate the MAPK signalling pathway, leading to the expression of inflammatory mediators and pro-inflammatory cytokines such as TNF-α and IL-6. The MAPK signalling pathway regulates inflammatory genes through phosphorylation of ERK, JNK and p38. The results showed that EA induced a significant increase in the levels of MAPK and NF-κB pathway-related proteins in the liver of SD rats, demonstrating that EA activated TLR4 in liver by inducing the release of LPS and pathogenic bacteria, leading to the activation of the MAPK and NF-κB signaling pathway and triggering the inflammatory response.

Inflammasome is associated with intestinal barrier integrity, microbial composition and liver injury[18]. Inflammasome activation is activated by endogenous or exogenous danger signals via TLR[53]. Palmitic acid induced massive release of LPS and stimulated NLRP3 inflammasome activation through the TLR4-NF-κB signal pathway in hepatic stellate cells[54]. The inflammatory response is an inducer of multiple types of diseases triggered by TFAs, but the exact mechanism is not clear. As inflammasome is involved in the body's defence response to various pathogenic stimuli, abnormalities in the NLRP3 inflammasome is responsible for the pathogenesis of several inflammatory diseases. Therefore, the effect of EA on NLRP3 inflammasome activation was investigated in rat liver. The results of H&E staining and ALT and AST assays in rats demonstrated that EA induced the development of inflammatory responses in the rat liver. The mRNA levels of *NLRP3*, *ASC*, *caspase-1* and *IL-1β* were significantly increased in the liver of EA-induced groups compared to the CON group, and their protein expression levels were also increased in a dose-dependent manner. ELISA results showed that EA induced a significant release of liver IL-1β, IL-18, IL-6 and TNF-α inflammatory factors. The present study showed that EA activated the NLRP3 inflammasome in the liver of SD rats, accompanied by the release of inflammatory factors. Further investigation of the molecular mechanisms underlying the NLRP3 inflammasome associated with the gut-liver axis may provide important insights into the identification of potential therapeutic targets for the treatment of liver and intestinal diseases[55].

Overall, EA caused chronic liver injury by inducing LPS release and translocation of pathogenic bacteria in the rat intestine. The intestinal barrier was disrupted, which led to the disruption of the gut-liver axis. This caused the translocation LPS into the circulatory system, which activated liver intrinsic immunity in combination with TLR4. Subsequently, the NF-κB and the MAPK signalling pathway were regulated in the liver through activation of the TLR4-MyD88 pathway, and NLRP3 inflammasome activation was ultimately induced.

Conflict of interest

The authors declare that there is no conflict of interests.

Acknowledgments

This work was supported by fund from the National Natural Science Foundation of China (32172322), Shandong Provincial Natural Science Foundation（ZR2023QC291), and Shandong Traditional Chinese Medicine Technology Project (Q-2023130). The authors gratefully acknowledge the fund support.

References

[1] Y. Hirata, A. Inoue, S. Suzuki, et al., *Trans*-fatty acids facilitate DNA damage-induced apoptosis through the mitochondrial JNK-Sab-ROS positive feedback loop, Sci. Rep. 10(1) (2020) 2743. https://doi.org/10.1038/S41598-020-59636-6.

[2] N. Gotoh, S. Kagiono, K. Yoshinaga, et al., Study of *trans* fatty acid formation in oil by heating using model compounds, J. Oleo Sci. 67(3) (2018) 273-281. https://doi.org/10.5650/jos.ess17209.

[3] A.B. Oteng, S. Kersten, Mechanisms of action of *trans* fatty acids, Adv. Nutr. 11(3) (2020) 697-708. https://doi.org/10.1093/advances/nmz125.

[4] A.B. Oteng, A. Bhattacharya, S. Brodesser, et al., Feeding Angptl4$^{-/-}$ mice *trans* fat promotes foam cell formation in mesenteric lymph nodes without leading to ascites, J. Lipid Res. 58(6) (2017) 1100-1113. https://doi.org/10.1194/jlr.M074278.

[5] A. Sauvat, G. Chen, K. Muller, et al., *Trans*-fats inhibit autophagy induced by saturated fatty acids, EBioMedicine 30 (2018) 261-272. https://doi.org/10.1016/j.ebiom.2018.03.028.

[6] H. Ka, B. Yi, M.J. Kim, et al., Effects of cis oleic and *trans* elaidic acids on oxidative stability in riboflavin and chlorophyll photosensitized oil-in-water emulsions, Food Sci. Food Biotechnol. 24(5) (2015) 1645-1648. https://doi.org/10.1007/s10068-015-0213-x.

[7] K. Kuhnt, M. Baehr, C. Rohrer, et al., *Trans* fatty acid isomers and the *trans*-9/*trans*-11 index in fat containing foods, Eur. J. Lipid Sci. Technol. 113(10) (2011) 1281-1292. https://doi.org/10.1002/ejlt.201100037.

[8] R. Ganguly, R. LaVallee, T.G. Maddaford, et al., Ruminant and industrial *trans*-fatty acid uptake in the heart, J. Nutr. Biochem. 31 (2016) 60-66. https://doi.org/10.1016/j.jnutbio.2015.12.018.

[9] I.A. Brouwer, A.J. Wanders, M.B. Katan, Effect of animal and industrial *trans* fatty acids on HDL and LDL cholesterol levels in humans-a quantitative review, PLoS One 5(3) (2010) e9434. https://doi.org/10.1371/journal.pone.0009434.

[10] T. Okamura, Y. Hashimoto, S. Majima, et al., *Trans* fatty acid intake induces intestinal inflammation and impaired glucose tolerance, Front. Immunol. 12 (2021) 669672. https://doi.org/10.3389/fimmu.2021.669672.

[11] Y. Ge, W. Liu, H. Tao, et al., Effect of industrial *trans*-fatty acids-enriched diet on gut microbiota of C57BL/6 mice, Eur. J. Nutr. 58(7) (2019) 2625-2638. https://doi.org/10.1007/s00394-018-1810-2.

[12] R.G. Visschers, M.D. Luyer, F.G. Schaap, et al., The gut-liver axis, Curr. Opin. Clin. Nutr. Metab. Care 16(5) (2013) 576-581. https://doi.org/10.1097/MCO.0b013e32836410a4.

[13] K. Allen, H. Jaeschke, B.L. Copple, Bile acids induce inflammatory genes in hepatocytes: a novel mechanism of inflammation during obstructive cholestasis, Am. J. Pathol. 178(1) (2011) 175-186. https://doi.org/10.1016/j.ajpath.2010.11.026.

[14] N.P. Woodcock, J. Robertson, D.R. Morgan, et al., Bacterial translocation and immunohistochemical measurement of gut immune function, J. Clin. Pathol. 54(8) (2001) 619-623. https://doi.org/10.1136/jcp.54.8.619.

[15] S. de Minicis, C. Rychlicki, L. Agostinelli, et al., Dysbiosis contributes to fibrogenesis in the course of chronic liver injury in mice, Hepatology 59(5) (2014) 1738-1749. https://doi.org/10.1002/hep.26695.

[16] J. Sabino, S. Vieira-Silva, K. Machiels, et al., Primary sclerosing cholangitis is characterised by intestinal dysbiosis independent from IBD, Gut 65(10) (2016) 1681-1689. https://doi.org/10.1136/gutjnl-2015-311004.

[17] N. Akhter, A. Hasan, S. Shenouda, et al., TLR4/MyD88-mediated CCL2 production by lipopolysaccharide (endotoxin): implications for metabolic inflammation, J. Diabetes Metab. Disord. 17(1) (2018) 77-84. https://doi.org/10.1007/s40200-018-0341-y.

[18] J. Henao-Mejia, E. Elinav, C. Jin, et al., Inflammasome-mediated dysbiosis regulates progression of NAFLD and obesity, Nature 482(7384) (2012) 179-185. https://doi.org/10.1038/nature10809.

[19] A. Wree, M.D. McGeough, M.E. Inzaugarat, et al., NLRP3 inflammasome driven liver injury and fibrosis: roles of IL-17 and TNF in mice, Hepatology 67(2) (2018) 736-749. https://doi.org/10.1002/hep.29523.

[20] K. Schroder, J. Tschopp, The inflammasomes, Cell 140(6) (2010) 821-832. https://doi.org/10.1016/j.cell.2010.01.040.

[21] M. Minemura, Y. Shimizu, Gut microbiota and liver diseases, World J. Gastroenterol. 21(6) (2015) 1691-1702. https://doi.org/10.3748/wjg.v21.i6.1691.

[22] P. Chen, P. Starkel, J.R. Turner, et al., Dysbiosis-induced intestinal inflammation activates tumor necrosis factor receptor I and mediates alcoholic liver disease in mice, Hepatology 61(3) (2015) 883-894. https://doi.org/10.1002/hep.27489.

[23] L. de Brito Medeiros, S. Alves, R. de Bessa, et al., Ruminant fat intake improves gut microbiota, serum inflammatory parameter and fatty acid profile in tissues of Wistar rats, Sci. Rep. 11(1) (2021) 18963. https://doi.org/10.1038/s41598-021-98248-6.

[24] H. Liu, B. Nan, C. Yang, et al., Elaidic acid induced NLRP3 inflammasome activation via ERS-MAPK signaling pathways in kupffer cells, Biochim. Biophys. Acta. Mol. Cell Biol. Lipids 1867(1) (2022) 159061. https://doi.org/10.1016/j.bbalip.2021.159061.

[25] S.H. Luo, W. Xiao, X.J. Wei, et al., *In vitro* evaluation of cytotoxicity of silver-containing borate bioactive glass, J. Biomed. Mater. Res. Part B 95(2) (2010) 441-448. https://doi.org/10.1002/jbm.b.31735.

[26] T.P. Bui, J. Ritari, S. Boeren, et al., Production of butyrate from lysine and the amadori product fructoselysine by a human gut commensal, Nat. Commun. 6 (2015) 10062. https://doi.org/10.1038/ncomms10062.

[27] H.Z. Zhu, Y.D. Liang, Q.Y. Ma, et al., Xiaoyaosan improves depressive-like behavior in rats with chronic immobilization stress through modulation of the gut microbiota, Biomed. Pharmacother. 112 (2019) 108621. https://doi.org/10.1016/J.Biopha.2019.108621.

[28] F.R. Ponziani, S. Bhoori, C. Castelli, et al., Hepatocellular carcinoma is associated with gut microbiota profile and inflammation in nonalcoholic fatty liver disease, Hepatology 69(1) (2019) 107-120. https://doi.org/10.1002/hep.30036.

[29] F.D. Urnov, A path to efficient gene editing, Nat. Med. 24(7) (2018) 899-900. https://doi.org/10.1038/s41591-018-0110-y.

[30] B.D. Needham, S.M. Carroll, D.K. Giles, et al., Modulating the innate immune response by combinatorial engineering of endotoxin, Proc. Natl. Acad. Sci. U.S.A. 110(4) (2013) 1464-1469. https://doi.org/10.1073/pnas.1218080110.

[31] T. Vatanen, A.D. Kostic, E. d'Hennezel, et al., Variation in microbiome LPS immunogenicity contributes to autoimmunity in humans, Cell 165(6) (2016) 1551. https://doi.org/10.1016/j.cell.2016.05.056.

[32] Y. Litvak, M.X. Byndloss, R.M. Tsolis, et al., Dysbiotic proteobacteria expansion: a microbial signature of epithelial dysfunction, Curr. Opin. Microbiol. 39 (2017) 1-6. https://doi.org/10.1016/j.mib.2017.07.003.

[33] Z.P. Gao, H. Wu, K.Q. Zhang, et al., Protective effects of grape seed procyanidin extract on intestinal barrier dysfunction induced by a long-term high-fat diet, J. Funct. Foods 64 (2020) 103663. https://doi.org/10.1016/J.Jff.2019.103663.

[34] C.S. Wang, W.B. Li, H.Y. Wang, et al., VSL#3 can prevent ulcerative colitis-associated carcinogenesis in mice, World J. Gastroenterol. 24(37) (2018) 4254-4262. https://doi.org/10.3748/wjg.v24.i37.4254.

[35] Y.Y. Lam, C.W. Ha, C.R. Campbell, et al., Increased gut permeability and microbiota change associate with mesenteric fat inflammation and metabolic dysfunction in diet-induced obese mice, PLoS One 7(3) (2012) e34233. https://doi.org/10.1371/journal.pone.0034233.

[36] Y. Hua, R. Fan, L. Zhao, et al., *Trans*-fatty acids alter the gut microbiota in high-fat-diet-induced obese rats, Br. J. Nutr. 124(12) (2020) 1251-1263. https://doi.org/10.1017/S0007114520001841.

[37] Q. Zhang, H. Yu, X. Xiao, et al., Inulin-type fructan improves diabetic phenotype and gut microbiota profiles in rats, PeerJ 6 (2018) e4446. https://doi.org/10.7717/peerj.4446.

[38] V.R. Figliuolo, L.M. Dos Santos, A. Abalo, et al., Sulfate-reducing bacteria stimulate gut immune responses and contribute to inflammation in experimental colitis, Life Sci. 189 (2017) 29-38. https://doi.org/10.1016/j.lfs.2017.09.014.

[39] C. Petersen, R. Bell, K.A. Kiag, et al., T cell-mediated regulation of the microbiota protects against obesity, Science 365(6451) (2019) eaat9351. https://doi.org/10.1126/science.aat9351.

[40] A. Miranda-Ribera, M. Ennamorati, G. Serena, et al., Exploiting the zonulin mouse model to establish the role of primary impaired gut barrier function on microbiota composition and immune profiles, Front. Immunol. 10 (2019) 2233. https://doi.org/10.3389/fimmu.2019.02233.

[41] C. Zhang, M. Zhang, X. Pang, et al., Structural resilience of the gut microbiota in adult mice under high-fat dietary perturbations, ISME J. 6(10) (2012) 1848-1857. https://doi.org/10.1038/ismej.2012.27.

[42] C. Li, Y.H. Zhang, Y.T. Ge, et al., Comparative transcriptome and microbiota analyses provide new insights into the adverse effects of industrial *trans* fatty acids on the small intestine of C57BL/6 mice, Eur. J. Nutr. 60(2) (2021) 975-987. https://doi.org/10.1007/s00394-020-02297-y.

[43] H. Zeng, J. Liu, M.I. Jackson, et al., Fatty liver accompanies an increase in lactobacillus species in the hind gut of C57BL/6 mice fed a high-fat diet, J. Nutr. 143(5) (2013) 627-631. https://doi.org/10.3945/jn.112.172460.

[44] M. Centanni, S. Turroni, S. Rampelli, et al., *Bifidobacterium animalis* ssp. *lactis* BI07 modulates the tumor necrosis factor alpha-dependent imbalances of the enterocyte-associated intestinal microbiota fraction, FEMS Microbiol. Lett. 357(2) (2014) 157-163. https://doi.org/10.1111/1574-6968.12515.

[45] A. Albillos, A. de Gottardi, M. Rescigno, The gut-liver axis in liver disease: pathophysiological basis for therapy, J. Hepatol. 72(3) (2020) 558-577. https://doi.org/10.1016/j.jhep.2019.10.003.

[46] W. Jiang, N. Wu, X. Wang, et al., Dysbiosis gut microbiota associated with inflammation and impaired mucosal immune function in intestine of humans with non-alcoholic fatty liver disease, Sci. Rep. 5 (2015) 8096. https://doi.org/10.1038/srep08096.

[47] I. Hritz, P. Mandrekar, A. Velayudham, et al., The critical role of toll-like receptor (TLR) 4 in alcoholic liver disease is independent of the common TLR adapter MyD88, Hepatology 48(4) (2008) 1224-1231. https://doi.org/10.1002/hep.22470.

[48] N. Qin, F. Yang, A. Li, et al., Alterations of the human gut microbiome in liver cirrhosis, Nature 513(7516) (2014) 59-64. https://doi.org/10.1038/nature13568.

[49] D. Feng, H. Zhang, X. Jiang, et al., Bisphenol a exposure induces gut microbiota dysbiosis and consequent activation of gut-liver axis leading to hepatic steatosis in CD-1 mice, Environ. Pollut. 265(Pt A) (2020) 114880. https://doi.org/10.1016/j.envpol.2020.114880.

[50] S.H. Lee, Intestinal permeability regulation by tight junction: implication on inflammatory bowel diseases, Intest. Res. 13(1) (2015) 11-18. https://doi.org/10.5217/ir.2015.13.1.11.

[51] Q. Zhang, M.J. Lenardo, D. Baltimore, 30 years of NF-κB: a blossoming of relevance to human pathobiology, Cell 168(1/2) (2017) 37-57. https://doi.org/10.1016/j.cell.2016.12.012.

[52] R.H. Du, J. Tan, N. Yan, et al., Kir6.2 knockout aggravates lipopolysaccharide-induced mouse liver injury via enhancing NLRP3 inflammasome activation, J. Gastroenterol. 49(4) (2014) 727-736. https://doi.org/10.1007/s00535-013-0823-0.

[53] H.B. Yu, B.B. Finlay, The caspase-1 inflammasome: a pilot of innate immune responses, Cell Host Microbe. 4(3) (2008) 198-208. https://doi.org/10.1016/j.chom.2008.08.007.

[54] Z. Dong, Q. Zhuang, M. Ning, et al., Palmitic acid stimulates NLRP3 inflammasome activation through TLR4-NF-κB signal pathway in hepatic stellate cells, Ann. Transl. Med. 8(5) (2020) 168. https://doi.org/10.21037/atm.2020.02.21.

[55] J. Wang, R. Dong, S. Zheng, Roles of the inflammasome in the gut-liver axis (review), Mol. Med. Rep. 19(1) (2019) 3-14. https://doi.org/10.3892/mmr.2018.9679.